

Z_n symmetry in the vortex muon decay

Pengcheng Zhao*

School of Physics and Astronomy, Sun Yat-sen University, 519082 Zhuhai, China

(Dated: November 2, 2022)

Polarization of a vortex state fermion has rich structure due to the nontrivial momentum distribution of wave function. This larger freedom provides an unique opportunity to prepare fermions in exotic polarized states, which do not exist for plane-wave state fermions. Based on the so called spin-orbit state which was studied both theoretically and experimentally, we put forward a peculiar vortex muon whose polarization exhibits Z_n symmetry and study its decay. We investigate the azimuthal distribution of the emitted electrons and find that it exhibits the same symmetry (Z_n) as the initial state.

I. INTRODUCTION

Physics of particles prepared in non-plane-wave states represents a fascinating cross disciplinary topic which attracts much attention [1, 2]. One particularly interesting class of none-plane wave states is vortex beams. The state carries non-zero orbital angular momentum (OAM) with respect to the propagation direction. Wave functions of the kind of states are always proportional to a spiral phase factor: $\psi(\mathbf{r}) = \psi(\rho, \phi, z) \propto \exp(il\phi)$, where ρ, ϕ are polar transverse coordinates, z is longitudinal coordinate and l is the integer topological charge. The topological charge acts as an important parameter to determine total angular momentum (TAM) of the state ($\hbar l$ is exactly the OAM for scalar field) and also represents an additional degree of freedom which specifies a peculiar series of non-plane-wave states. Optical vortex beams have been studied since the last decade of the 20th century [4–9], vortex electrons have been produced ten years ago [10], and recently neutrons [11] and atoms [12] also have been put into vortex states. They have already found numerous applications in manipulation of matter, quantum communication, microscopy and so on [13–22]. For fundamental physics, it is interesting to investigate how particles in vortex states will modify standard scattering processes [23–32]. Recently, the vortex muon decay has been calculated [33]. The spectral-angular distribution of the emitted electron displays several features which are different from plane-wave muons.

In addition to the OAM, vortex states bring novel polarization opportunities. In contrast to plane waves which are described by constant polarization vectors (for photons) or spin vectors (for fermions), polarization of vortex light or fermions can be described with a continuous *field* of polarization parameters. The much larger freedom of defining a polarization state allows for exotic polarizations which would be unthinkable for plane waves. Particularly, we get TAM eigenstates with rotational-symmetric polarization field. For these kind of states, the only thing that breaks rotation symmetry is the phase distribution, which increases evenly according to the topological charge when we rotate the state by certain axis. Vortex states with rotational-asymmetric polarization field are not TAM eigenstates and have more complicated structure.

A variety of polarized vortex light beams have been generated with a special spatial light modulator accompanied by well-designed optical device series [34, 35]. The experiments utilize interference of two Laguerre-Gaussian (LG) beams or Hermite-Gaussian (HG) beams with different quantum numbers and different constant polarization modes to acquire light beams with nonconstant polarization modes. For example, radially polarized beams and azimuthally polarized beams which are rotational-symmetric are generated, and beams named as anti-vortices with peculiar periodic azimuthal polarization distribution which break the rotation symmetry but reserve certain Z_n symmetry are also generated [35]. These kind of states are also called spin-orbit states because it describes states with correlated spin and orbital angular momentum [36]. Light beams prepared in such states have unusual electromagnetic field distribution and have been suggested to have applications in polarization spectroscopy, linear electron beam accelerator and data storage [37–39]. Generation of spin-orbit fermion states have also been proposed for electron and neutron [40, 41]. One method is to propagate an electron or neutron wave packet, which has zero topological charge and constant spin distribution along z direction, through a quadrupole magnetic field whose field intensity vectors locate in one plane and are orthogonal to z direction. The generated spin-orbit state is coherent superposition of two states with different topological charges (difference between them can only be one) and opposite polarizations. It is proposed for electron in [40] and expanded for neutron in [41]. Another method is to prepare a state which has zero topological charge and is coherent superposition of both spin up and spin down states, and then propagates it through a magnetic

* zhaopch5@mail2.sysu.edu.cn

spiral phase plate (mSPP)[41]. If the mSPP is appropriately magnetized, only spin up (or spin down) component changes its topological charge according to the winding number of the mSPP. By this method, we can get spin-orbit states with arbitrary topological charge components. It is proposed in [41] for neutron and well-designed sequential quadrupole chain is also proposed to increase range of maximal entanglement. In principle, both the two methods can be applied to any other fermion as long as its beam is stable enough. For example, it should be realizable for muon beams with appropriately high energy. Other method like using ‘‘lattice of optical vortices’’ prism pairs to put spin-orbit state into lattices is also proposed. Lattices of spin-orbit neutron state has been claimed to be realized experimentally[42], but the image is not distinct enough. Fortunately, similar experiment for light beam gives nice result [43], which shows the feasibility of the method. Spin distribution of the anticipant spin-orbit fermion states may also be rotational symmetric (for example, cylindrically polarized states, azimuthally polarized states, radially polarized states, hedgehog skyrmion states and spiral skyrmion states) or exhibit Z_n symmetry (for example, hybrid polarized states and quadrupole spin-orbit states) as light beams do [41].

As is realized for photon and suggested for fermions, one can imagine a vortex fermion state, whose local polarization parameters change in the transverse plane as functions of the radial coordinate r and azimuthal coordinate φ . They can exhibit a periodic dependence on φ and thus gives vortex states which exhibit Z_n symmetry. This kind of state is expected to be generated by the methods discussed above with well-designed experimental installations. Instead of continuous azimuthal rotations, such a peculiar fermion state is invariant under its discrete subgroup. It represents yet another adjustable degree of freedom whose physical significance and potential application remain essentially unknown up to now. In this paper, we explore some properties of the new degree of freedom, which is specialized by positive integer number n from Z_n symmetry of the state, in a simple setting: decay of the vortex muon prepared in a polarization state with Z_n symmetry. Our previous work on vortex muon decay [33] assumed the polarization state to be invariant under continuous azimuthal rotations and it resulted in electron distribution that is also rotational symmetric. In that paper, we detailedly discussed kinematical characteristics of vortex muon decay. Now, we explore the case that the vortex muon state exhibits Z_n symmetry and discuss whether the Z_n symmetry will remain for the final state after decay of the polarized vortex muon by exploring angular characteristics.

The paper is organized as follows. In section II, we describe vortex states with Z_n symmetry. In section III, we give general formulas for calculation of vortex muon decay at tree level. In section IV, we prove that the initial state and emitted electron distribution for polarized vortex muon decay exhibits the same Z_n symmetry and give some examples. In section V, we draw the conclusions. In this paper, the natural units are used. Average 3-momentum direction of initial state is chosen to be z axis. We use symbol \vec{r} to represent transverse 2D vectors, \mathbf{r} to represent 3D vectors and r^μ to represent 4D vectors.

II. VORTEX MUON STATE WITH Z_n SYMMETRY

A. From plane wave state to vortex state

As a fermion, single muon state is given by the solution of the Dirac equation. In the standard representation, the plane wave muon state in coordinate space is:

$$\psi^{PW}(x) = u(p^\mu, s^\nu) e^{-iEt + i\mathbf{p}\cdot\mathbf{x}}, \quad (1)$$

where $p^\mu = (E, \mathbf{p})$ is the 4-momentum of muon, E is muon energy, \mathbf{p} is muon 3-momentum, s^ν represents spin of muon. The spinor can be written as

$$u(p^\mu, s^\nu) = \frac{1}{\sqrt{2E}} \begin{pmatrix} \sqrt{E+m} w \\ \sqrt{E-m} \boldsymbol{\sigma} \cdot \mathbf{n} w \end{pmatrix}, \quad w = \begin{pmatrix} \cos \frac{\alpha}{2} \\ \sin \frac{\alpha}{2} e^{i\delta} \end{pmatrix}. \quad (2)$$

m is muon mass, \mathbf{n} is unit vector along muon's direction of motion. Polarization of the state is described by the spinor with two free parameters α and δ or 4-vector s^ν . There is one-to-one correspondence between them. Polarization 4-vector of completely polarized muon is $s^\nu = (S^0, \mathbf{S}) = (\gamma\beta(\mathbf{n} \cdot \mathbf{s}), \mathbf{s} + (\gamma - 1)(\mathbf{n} \cdot \mathbf{s})\mathbf{n})$, where \mathbf{s} is unit vector in muon spin direction in the rest frame, β is muon speed and $\gamma = 1/\sqrt{1 - \beta^2}$ [44].

As for the vortex state, it can be described by linear combination of many different plane waves. The most simple vortex state is the Bessel vortex state. The wave function of Bessel fermion state is written as [23, 45]

$$\begin{aligned} \psi_{E,\kappa,l}^V(x) &= e^{-iEt + iqz} \int \frac{d^2\vec{k}}{(2\pi)^2} a_{\kappa l}(\vec{k}) u(p^\mu, s^\nu) e^{i\vec{k}\cdot\vec{\rho}} \\ a_{\kappa l}(\vec{k}) &= (-i)^l \sqrt{\frac{2\pi}{\kappa}} \delta(|\vec{k}| - \kappa) e^{il\varphi_p}, \end{aligned} \quad (3)$$

where $p^\mu = (E, \vec{k}, q)$ is 4-momentum of each plane wave component, E is energy, $\vec{k} = (|\vec{k}|, \varphi_p)$ is the transverse 2-dimensional projection of p^μ , q is longitudinal momentum, $x^\mu = (t, \vec{\rho}, z)$ is the 4-vector in coordinate space, t is time, $\vec{\rho} = (|\vec{\rho}|, \varphi_r)$ is the transverse 2-dimensional projection of x^μ , z is longitudinal space coordinate, κ is transverse momenta modulus, l is topological charge (integer quantum number for vortex) of Bessel type vortex state. In the momentum space, its distribution forms a circle that is orthogonal to propagation direction and all the momentum vectors form a circular cone as Fig. 1 shows. Three quantum numbers E , κ , and l uniquely determine the state. Other vortex state like LG state can be regarded as superposition of many Bessel type vortex states. Since its simplicity, we just discuss Bessel type vortex state in this paper.

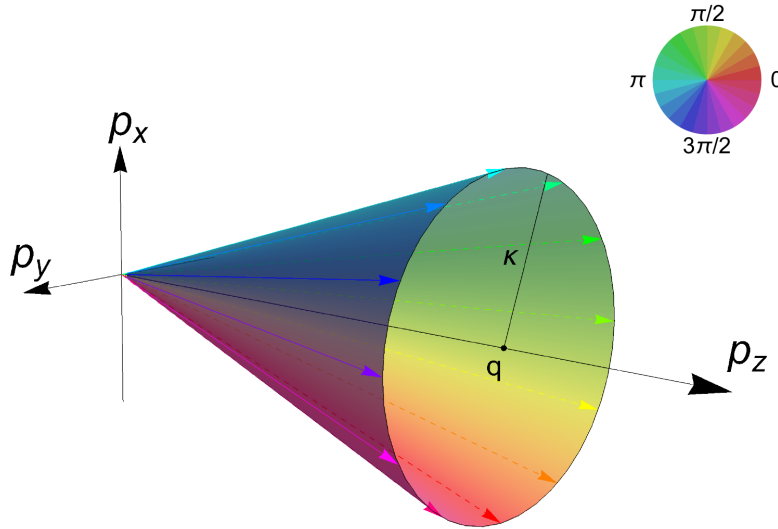


Figure 1. Bessel vortex state with $l = 1$. It is a monochromatic state. The black circle with radius κ gives distribution in momentum space. All the momentum vectors form a circular cone. Phase factors of plane wave components changes $2\pi l$ in one circle (different phases are shown by different colors) and l acts as vortex quantum number (topological charge) of the state. q is length of average momentum. κ is length of transverse momentum for all plane wave components, which also acts as transverse quantum number of the state.

Note that, two free parameters α and δ in the spinor $u(p^\mu, s^\nu)$ for different plane wave components can be the same or different. For the case that they keep the same, the state must be rotational-symmetric[33, 46, 47]. For the case that we have angular dependent parameters $\alpha(\varphi_p)$ and $\delta(\varphi_p)$, the state can have diverse structures. It's these dependence that indicate the possibility of constructing vortex state with Z_n symmetry.

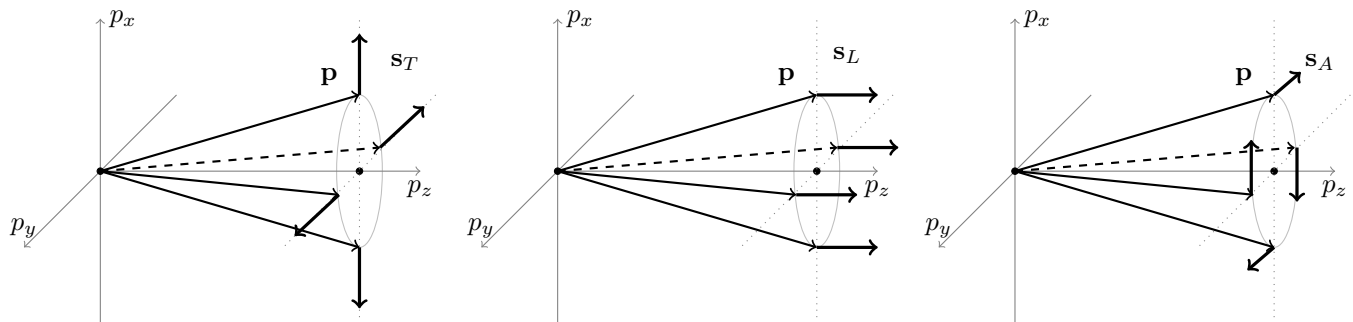


Figure 2. Three classes of basic vectors in momentum space for describing polarization of vortex particles: transverse basic vectors (left), longitudinal basic vectors (center), and azimuthal basic vectors (right). Every plane wave component has polarization vector \mathbf{s} that is combined by three orthogonal basic vectors from different classes.

Since \mathbf{S} is a three-dimensional vector, it is convenient to choose three basic vectors to represent it. The three unit vectors for every plane wave component with momentum \mathbf{p} are selected as $(\pi/2, \varphi_p)$ (transverse), $(0, 0)$ (longitudinal) and $(\pi/2, \varphi_p - \pi/2)$ (azimuthal), which are expressed in the spherical coordinate. They are visualized in Fig.2 and

labeled as $\mathbf{s}_T, \mathbf{s}_L, \mathbf{s}_A$ respectively. Generally, for arbitrary polarized vortex state, every plane wave component in it has its own 4-vector $s^\nu = (S^0, \mathbf{S})$:

$$\begin{aligned} S^0 &= \gamma\beta (\mathbf{n} \cdot \mathbf{s}) = \beta (\mathbf{n} \cdot \mathbf{S}), \\ \mathbf{S} &= a_p \mathbf{s}_T + b_p \mathbf{s}_L + c_p \mathbf{s}_A, \end{aligned} \quad (4)$$

where a_p, b_p, c_p are functions of φ_p . They satisfy normalization condition (seeing Appendix A)

$$(a_p \sin \theta_0 + b_p \cos \theta_0)^2 + \gamma^2 (a_p \cos \theta_0 - b_p \sin \theta_0)^2 + \gamma^2 c_p^2 = \gamma^2, \quad (5)$$

where $\theta_0 = \arctan(\kappa/q)$ is conical angle of vortex muon in momentum space. This equation means that the three parameters a_p, b_p, c_p are not independent and it is coincident with the fact that plane wave muon has two degrees of spin freedom.

Polarization of plane wave muon is described by one constant vector. By combination of different plane waves with different momenta and polarizations, the spin distribution of none-plane wave fermion can have complicated structure. Polarized vortex muon state can be designed with azimuthal-periodic structure, which exhibits Z_n symmetry. This is what we call ‘‘vortex muon state with Z_n symmetry’’, which corresponds to the case that parameters a_p, b_p, c_p behave as periodic functions of φ_p with period $2\pi/n$ (n can be any positive integer). Integer n of Z_n symmetry is another peculiar number that specialize the muon state except for muon energy E , transverse quantum number κ and topological charge l .

B. Visualization of vortex muon with Z_n symmetry

To visualize the polarized vortex photon, we can use the classical electrodynamics quantities: the electric and magnetic field. But there is no such kind of classical quantity for fermions. In quantum mechanics, we describe the polarization of a plane wave fermion with spin. Under non-relativistic limitation, we can use spin field to visualize the polarization of vortex muon with Z_n symmetry.

To give a simple example, we apply paraxial approximation, which means the conical angle θ_0 is much small. Then the monochromatic muon states we discuss can approximately be eigenstate of OAM and spin operator simultaneously. Here, we just use this approximation to facilitate the visualization of the spin field of our state. Later calculation about muon decay is not limited with it.

It is convenient to set a_p, b_p and c_p instead of $\alpha(\varphi_p)$ and $\delta(\varphi_p)$ as periodic functions of φ_p to construct the kind of vortex muon we need. Relations between the two groups of parameters are given in Appendix A. Particularly, with non-relativistic limitation and the paraxial approximation ($\sin \theta_0 \rightarrow 0$ and $\cos \theta_0 \rightarrow 1$), we choose these special cases:

$$b_p = \gamma b, \quad a_p = \sqrt{1 - b^2} \cos n\varphi_p, \quad c_p = \sqrt{1 - b^2} \sin n\varphi_p, \quad (6)$$

with $-1 < b < 1$ and n being a positive integer. Then integral of the state in Eq.(3) gives

$$\psi^V(x) = \sqrt{\frac{\kappa}{2\pi}} \left(\begin{array}{c} \sqrt{\frac{b+1}{2}} J_l(\kappa\rho) \\ \sqrt{\frac{1-b}{2}} J_{l+1-n}(\kappa\rho) e^{i[(1-n)\varphi_r]} \end{array} \right) e^{il\varphi_r} e^{-iEt+iqz}, \quad (7)$$

where J_l is Bessel functions of first kind with order l . The other two componets of spinor $u(p^\mu, s^\nu)$ tend to 0 due to non-relativistic limitation and are ignored. Thus, we can describe the spin distribution in coordinate space with up and down type spinors

$$\begin{aligned} \psi^V(x) &= P_{up}(\rho, \varphi_r, z) |\uparrow\rangle + P_{down}(\rho, \varphi_r, z) |\downarrow\rangle \\ &= \frac{1}{N} \left(\sqrt{\frac{b+1}{2}} J_l(\kappa\rho) |\uparrow\rangle + \sqrt{\frac{1-b}{2}} J_{l+1-n}(\kappa\rho) e^{i[(1-n)\varphi_r]} |\downarrow\rangle \right) e^{il\varphi_r} e^{-iEt+iqz}, \end{aligned} \quad (8)$$

where

$$N = \sqrt{\frac{b+1}{2} J_l^2(\kappa\rho) + \frac{1-b}{2} J_{l+1-n}^2(\kappa\rho)}$$

is ρ -dependent coefficient. The spin field can be described by arrows filling all the space. The arrows are drawn by method of ‘‘Poincare sphere’’ according to difference between P_{up} and P_{down} [48].

For a specific case, we set $b = 0$. This gives the state with polarization 3-vector \mathbf{S} of every plane wave component all locating in the transverse plane in the momentum space. In the coordinate space, the spin distribution can be complicated. Its structure is fully determined by number l , κ and n . One example with $l = 12$ and $n = 3$ is showed in Fig.3. In the figure, we show the special concentric circles on which the arrows that represent spin locate in transverse plane or are orthogonal to the plane. They correspond to the cases that the two Bessel functions in Eq.(8) have the same modulus or one of the Bessel functions is equal to zero. In principle, there are an ocean of concentric circles. We draw four smallest ones in the figure. The center of the circles is singularity of vortex state. At points in the empty space, either in the smallest circle or between adjacent concentric circles, the arrows have both transeverse and langitudinal components. The most notable feature of the figure is that the spin distribution is rotational-invariant about z axis under certain rotation angles, i.e. integer multiples of $2\pi/n$. This kind of symmetry is just Z_n symmetry we designed for our vortex state in momentum space.

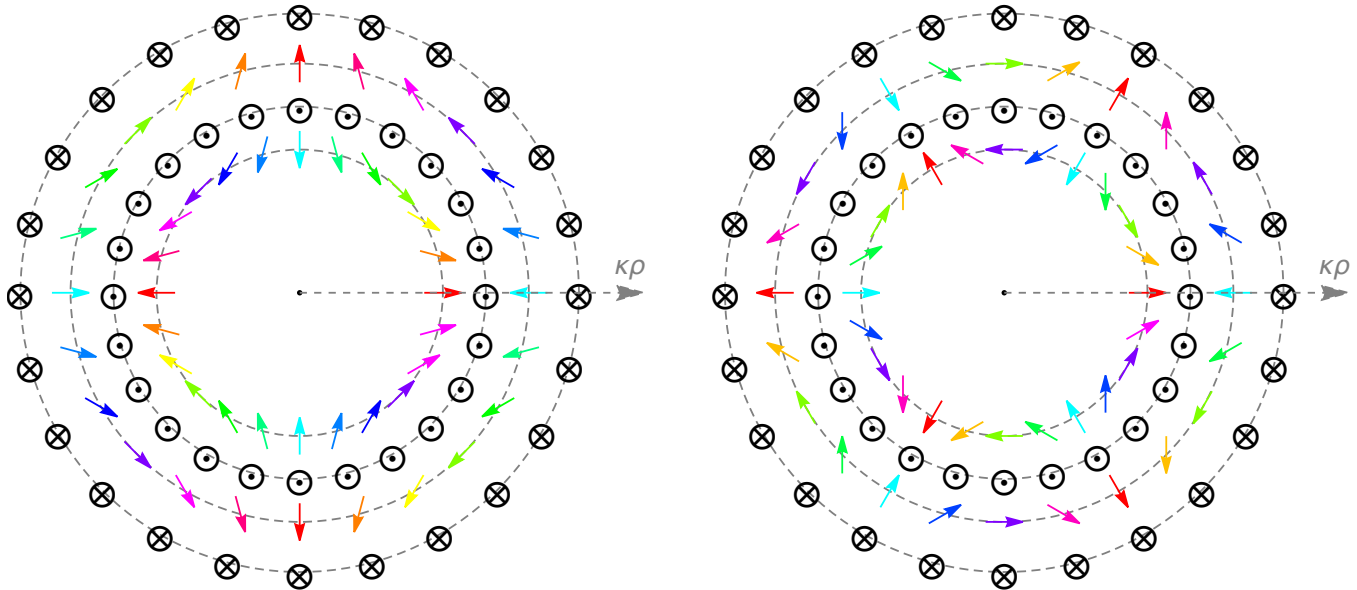


Figure 3. Coordinate-space spin distribution of state described in Eq. (8) in transverse plane in case that $b = 0$ and $l = 12$. $n = 2$ for left picture and $n = 3$ for right one. The arrows represent spin at every space point. Only arrows that are completely transverse or longitudinal are drawn. Radial length is not well-proportioned here. Different colors correspond to different direction in transverse plane and show clearly the Z_n symmetry (Z_2 for left side and Z_3 for right side). “ \odot ” and “ \otimes ” mean spin to z and opposite directions respectively.

III. MUON DECAY FROM PLANE WAVE CASE TO VORTEX CASE

To simplify the calculation, electron and neutrino masses are set to zero, and only tree level decay process is considered. Either the plane wave muon or the vortex muon that we consider are completely polarized. We review the plane wave muon decay first and then give formulas for the vortex muon decay.

A. Decay of the plane wave muon

The symbols we use here are showed as follows. The two constants m and G_F are muon mass and Fermi constant. The unit vector of z direction is \mathbf{n}_z . p^μ and k^μ are four-momentums of muon and electron. We write $p^\mu = E(1, \beta\mathbf{n})$, where E , β , \mathbf{n} are muon energy, muon speed and unit vector of muon direction of motion respectively. We write $k^\mu = E_e(1, \mathbf{n}_e)$ with $\mathbf{n}_e \cdot \mathbf{n}_z = \cos\theta_e$, where E_e , \mathbf{n}_e , θ_e are electron energy, unit vector of electron direction of motion and electron emission angle respectively. Electron moving direction is (θ_e, ϕ_e) .

The spectral-angular distribution for vortex muon is written as [33]

$$\begin{aligned} \frac{d\Gamma_{PW}}{dE_e d\Omega} &= \frac{G_F^2 E_e}{48\pi^4 E} \left\{ (pk)(3m^2 - 4(pk)) - m(sk)(m^2 - 4(pk)) \right\} \\ &= \frac{G_F^2 E_e}{48\pi^4 E} \left\{ [3m^2 EE_e(1 - \beta \mathbf{n} \cdot \mathbf{n}_e) - 4E^2 E_e^2(1 - \beta \mathbf{n} \cdot \mathbf{n}_e)^2] - mE_e(S^0 - \mathbf{S} \cdot \mathbf{n}_e)[m^2 - 4EE_e(1 - \beta \mathbf{n} \cdot \mathbf{n}_e)] \right\} \end{aligned} \quad (9)$$

The formula in curly brackets is a sum of two different terms. The first term corresponds to the unpolarized plane wave muon case. The second term corresponds to the modification of polarized case to unpolarized case. What should be noted is that the maximum energy of the emitted electron depends on the emission angle θ_e :

$$E_{em} = \frac{m^2}{2E(1 - \beta \mathbf{n} \cdot \mathbf{n}_e)}. \quad (10)$$

According to Eq. (9), we can get electron spectral-azimuthal distribution as function of E_e and ϕ_e at fixed θ_e . It will be axisymmetric around z axis, i.e. independent of azimuthal angle ϕ_e , if both \mathbf{n} and \mathbf{S} are parallel to z axis. Or else, it will be ϕ_e -dependent. If \mathbf{n} is parallel to z axis while \mathbf{S} is not, the dependence will be described by trigonometric functions of ϕ_e with frequency 1, i.e. $\cos \phi_e$ and $\sin \phi_e$. If \mathbf{n} is not parallel to z axis, the dependence will be described by trigonometric functions with both 1 and 2 frequencies, i.e. $\cos \phi_e$, $\sin \phi_e$, $\cos 2\phi_e$ and $\sin 2\phi_e$. Note that the axisymmetric contribution (*i.e.* constant term) always exist.

B. Decay of the vortex muon

Bessel type vortex muon is combination of equal-weight plane waves with azimuthally distributed phase factors. Its differential decay width is angular average of decay width of every plane wave components:

$$d\Gamma_V = \int \frac{d\varphi_p}{2\pi} d\Gamma_{PW}(\mathbf{p}). \quad (11)$$

If θ_e and θ_0 are fixed, the plane wave components' contribution to the spectral-angular distribution is classified into two classes by two characteristic electron energy: E_{e1} and E_{e2} [33]. Electrons with energy smaller than E_{e1} can be produced by any plane wave components, but electrons with energy bigger than E_{e1} and smaller than E_{e2} can only be produced by sectional components whose azimuthal angle φ_p runs over $(\phi_e - \tau, \phi_e + \tau)$. The two energies are expressed as

$$E_{e1} = \frac{m^2}{2E(1 - \beta \cos(\theta + \theta_0))} \quad \text{and} \quad E_{e2} = \frac{m^2}{2E(1 - \beta \cos(\theta - \theta_0))}. \quad (12)$$

And the critical angle τ satisfies

$$\cos \tau = \frac{(E_e - E_{e1})E_{e2} - (E_{e2} - E_e)E_{e1}}{E_e(E_{e2} - E_{e1})}. \quad (13)$$

The spectral-angular distribution for polarized vortex muon decay is written as [33]

$$\frac{d\Gamma_V}{dE_e d\Omega} = \frac{G_F^2 E_e}{48\pi^4 E} \int_{\phi_e - \tau}^{\phi_e + \tau} \frac{d\varphi_p}{2\pi} \left\{ [3m^2 EE_e(1 - \beta \mathbf{n} \cdot \mathbf{n}_e) - 4E^2 E_e^2(1 - \beta \mathbf{n} \cdot \mathbf{n}_e)^2] - mE_e(S^0 - \mathbf{S} \cdot \mathbf{n}_e)[m^2 - 4EE_e(1 - \beta \mathbf{n} \cdot \mathbf{n}_e)] \right\}. \quad (14)$$

For $E_{e1} < E_e < E_{e2}$, we have $0 < \tau < \pi$, while for $0 < E_e < E_{e1}$, just set $\tau \rightarrow \pi$.

We take modification of polarized case to unpolarized case out of Eq. (14):

$$\frac{d\Gamma_V^{mod}}{dE_e d\Omega} = \frac{G_F^2 E_e}{48\pi^4 E} \int_{\phi_e - \tau}^{\phi_e + \tau} \frac{d\varphi_p}{2\pi} \left\{ -mE_e(S^0 - \mathbf{S} \cdot \mathbf{n}_e)[m^2 - 4EE_e(1 - \beta \mathbf{n} \cdot \mathbf{n}_e)] \right\}. \quad (15)$$

The direction of unit vectors \mathbf{n} and \mathbf{n}_e are respectively (θ_0, φ_p) and (θ_e, ϕ_e) . Product of unit vectors in direction (θ_1, φ_1) and (θ_2, φ_2) is " $\cos \theta_1 \cos \theta_2 + \sin \theta_1 \sin \theta_2 \cos(\varphi_1 - \varphi_2)$ ". Then we get

$$\frac{d\Gamma_V^{mod}}{dE_e d\Omega} = \frac{G_F^2 m E_e^2}{48\pi^4 E} \int_{\phi_e - \tau}^{\phi_e + \tau} \frac{d\varphi_p}{2\pi} \left\{ [\beta(a_p \sin \theta_0 + b_p \cos \theta_0) - a_p(\mathbf{s}_T \cdot \mathbf{n}_e) - b_p(\mathbf{s}_L \cdot \mathbf{n}_e) - c_p(\mathbf{s}_A \cdot \mathbf{n}_e)][4EE_e(1 - \beta \mathbf{n} \cdot \mathbf{n}_e) - m^2] \right\}, \quad (16)$$

where

$$\begin{aligned}\mathbf{s}_T \cdot \mathbf{n}_e &= \sin \theta_e \cos(\varphi_p - \phi_e), \\ \mathbf{s}_L \cdot \mathbf{n}_e &= \cos \theta_e, \\ \mathbf{s}_A \cdot \mathbf{n}_e &= \sin \theta_e \sin(\varphi_p - \phi_e), \\ \mathbf{n} \cdot \mathbf{n}_e &= \cos \theta_e \cos \theta_0 + \sin \theta_e \sin \theta_0 \cos(\varphi_p - \phi_e).\end{aligned}$$

IV. ELECTRON DISTRIBUTION WITH Z_n SYMMETRY AFTER MUON DECAY

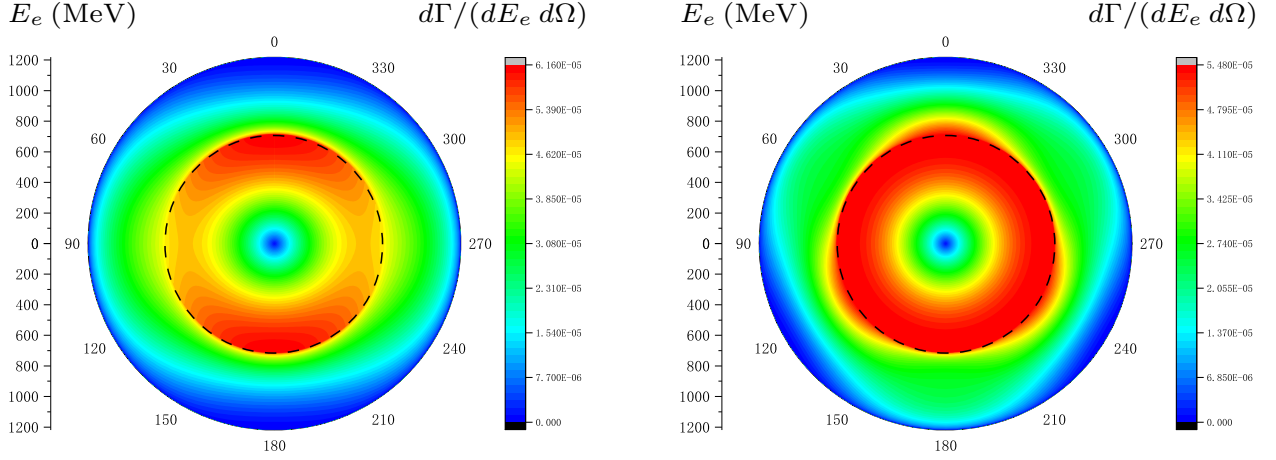


Figure 4. Contour map of spectral-azimuthal distribution at $\theta_e = \pi/60$ for emitted electron. The figures are drawn in polar coordinate system. Polar angle represents electron azimuthal angle ϕ_e and radial axis represents electron energy E_e . The contours with different colors represent dimensionless differential decay width $d\Gamma_V/(dE_e d\Omega)$ of muon decay. The black dashed circles correspond to cases of $E_e = E_{e1}$. The initial muon state is fixed by parameters: $E = 3.1 \text{ GeV}$, $\theta_0 = 0.01$, $l = 12$, $a_p = \gamma \cos n\varphi_p / \sqrt{\gamma^2 \cos^2 \theta_0 + \sin^2 \theta_0}$, $b_p = 0$ and $c_p = \sin n\varphi_p$ (Equation (5) is satisfied). The state exhibits Z_n symmetry. $n = 2$ for the left picture and $n = 3$ for the right picture.

We reconstruct the integral in Eq. (16) as

$$\frac{d\Gamma_V^{mod}}{dE_e d\Omega} = \frac{G_F^2 m E_e^2}{48\pi^4 E} \int_{\phi_e - \tau}^{\phi_e + \tau} \frac{d\varphi_p}{2\pi} \left\{ a_p \sum_{f=0}^2 x_f \cos[f(\varphi_p - \phi_e)] + b_p \sum_{g=0}^1 y_g \cos[g(\varphi_p - \phi_e)] + c_p \sum_{h=1}^2 z_h \sin[h(\varphi_p - \phi_e)] \right\}. \quad (17)$$

Here x_f , y_g and z_h are all independent of φ_p and ϕ_e . They are determined by parameters of the initial state and emitted electron. As the vortex muon state we consider exhibits Z_n symmetry, a_p , b_p and c_p must be periodic functions of φ_p with period $2\pi/n$ ($n = 1, 2, 3, \dots$). Thus they can be expanded as trigonometric series:

$$\frac{1}{2} A_0 + \sum_{\zeta=1}^{\infty} [A_n \cos(\zeta n\varphi_p) + B_n \sin(\zeta n\varphi_p)].$$

We will see later that this expansion extremely simplifies our discussion.

First, we look into the electrons with energy $0 < E_e < E_{e1}$, where all plane wave components contribute to the result and we set $\tau = \pi$ in Eq. (17). According to the orthogonality of trigonometric integration, we can get the result that the integrals of “ $\cos(\varphi_p - \phi_e)$ ”, “ $\cos[2(\varphi_p - \phi_e)]$ ”, “ $\sin(\varphi_p - \phi_e)$ ” and “ $\sin[2(\varphi_p - \phi_e)]$ ” in Eq. (17) work as filters to keep the same trigonometric term and filter all the other terms in periodic functions a_p , b_p , c_p . And reserved azimuthal distribution behaves with “ $\cos(\phi_e)$ ”, “ $\cos(2\phi_e)$ ”, “ $\sin(\phi_e)$ ” and “ $\sin(2\phi_e)$ ”. The terms independent of ϕ_e give constant azimuthal distribution. The final azimuthal distribution can get contribution from trigonometric functions with frequency 1 or 2 but no contribution from ones with bigger frequencies. It can only have Z_2 symmetry

or no Z_n symmetry, which both come from symmetry of initial state. Z_n symmetries with $n \geq 3$ can not be delivered to final state in this energy region.

Second, we look into the electrons with energy $E_{e1} < E_e < E_{e2}$, where only sectional plane wave components contribute to the result and we keep the formula of τ in Eq. (17). The τ , which satisfies Eq. (13), is a constant when initial muon and final electron state are fixed. This simplifies the integral. We insert integrals listed in Appendix B into Eq. (17). And then we can see that the integral with $\cos(\varphi_p - \phi_e)$ and $\cos[2(\varphi_p - \phi_e)]$ work as amplitude modulators to rescale the amplitudes in front of trigonometric series with different frequency, while the integral with $\sin(\varphi_p - \phi_e)$ and $\sin[2(\varphi_p - \phi_e)]$ work as amplitude and phase united modulators to rescale the amplitudes and change the modes between $\cos(\zeta n \phi_e)$ and $\sin(\zeta n \phi_e)$ at the same time. The characteristic of these integrals causes the final result of Eq. (17) keeping the frequencies of every trigonometric components in $a_p(\varphi_p)$, $b_p(\varphi_p)$, $c_p(\varphi_p)$, and thus the spectral-azimuthal distribution (as functions of ϕ_e) also shows Z_n symmetry as initial vortex muon state does for any positive integer number n .

Specially, examples are showed in Fig. 4. A black dashed circle at $E_e = E_{e1}$ is drawn for distinguishing of the two different energy regions in both pictures. In the left picture, the initial state exhibits Z_2 symmetry and we can see that the electron distribution also exhibits Z_2 symmetry no matter in the circle or outside the circle. This is consistent with our discussion above for $n \leq 2$. In the right picture, the initial state exhibits Z_3 symmetry and we can see that the electron distribution exhibits Z_3 symmetry outside the circle but is rotationally symmetric in the circle. This is also consistent with our discussion above for $n \geq 3$. In a global view, we can conclude that final electron distribution have the same Z_n symmetry with initial muon state for any positive integer n . And if initial state has no Z_n symmetry, the electron distribution will also has no Z_n symmetry.

Note that there is possibility that initial state with Z_n symmetry may results in azimuthal distribution of electron (in the cases that energy E_e and emission angle θ_e are fixed) with $Z_{n'}$ symmetry, where n' is integer multiple of n . But this is not a general result. It just corresponds to the case that the $\cos(n\phi_e)$ and $\sin(n\phi_e)$ terms disappear together for coincidental electron energy and emission angle. But it does not influence the final result, because all the possible electron energy and emission angle should be read in conjunction. Global electron azimuthal distribution can only exhibit the same Z_n symmetry as the initial state does.

The result is not difficult to be understood. To do it, we need to keep three prerequisites in mind:

- There is no interference between any plane wave components in vortex state. Square of M matrix for vortex muon decay can be deduced as angular average of M^2 for all plane wave components. This applies to all processes with only one vortex initial state [23]. Thus we can think of vortex muon decay by simply imagining superposition of decay of infinite plane wave muons whose momentums and polarizations are determined by vortex state.
- For the plane wave muon decay, the contribution from polarization modification (compared with unpolarized case) is proportional to polarization 4-vector, which is showed in Eq. (9). Thus we can reconstruct integral in Eq. (16) as integral of linear terms of φ_p -dependent weight factors (a_p , b_p and c_p), as showed in Eq. (17).
- Spectral-azimuthal distribution of plane wave muon decay has azimuthal dependence described by trigonometric functions with frequencies 1 and 2 if 3-momentum of the muon is not parallel to z axis for both unpolarized and polarized cases, which is discussed at last paragraph of Section III Part A. If we rotate the 3-momentum of the plane wave with certain angle around z axis, the azimuthal dependent distribution will rotate simultaneously with the same angle. But the shape of the distribution is not changed.

With the three prerequisites, we can understand contribution from unpolarized part and polarization modification part of vortex muon decay respectively. Sum of them is showed in Eq. (14) and the modification part is showed in Eq. (15). For angular average of unpolarized part, we have no φ_p -dependent weight factors and simply get equal weight superposition of azimuthal distributions that rotate along with rotating of plane wave 3-momentum. The rotation scans a full circle of 3-momentum since momentum distribution of vortex state is just a circle. Thus the result of the superposition is axisymmetric, which means it exhibits any Z_n symmetry. For angular average of polarization modification part, we have additional φ_p -dependent weight factors for the superposition. The distribution is modified by the weight factors which can be expanded as trigonometric series. If $0 < E_e < E_{e1}$, the trigonometric functions in the plane wave components distributions work as filters to trigonometric function components in the weight factors. Thus, only frequencies 1 (no Z_n symmetry) and 2 (Z_2) in trigonometric function components of the weight factors can survive in the result. The distribution will be axisymmetric if both of the frequencies do not exist. If $E_{e1} < E_e < E_{e2}$, the trigonometric functions in the plane wave components distributions work as phase and amplitude modulators to trigonometric function components of the weight factors. And the frequencies in trigonometric function components of the weight factors are not changed, which means the Z_n symmetry of the weight factors is kept. In summary, we get the result discussed in previous paragraphs and showed in Fig. 4. The same logic applies to other interactions as long as the three prerequisites are satisfied. Note that the frequencies in the third prerequisite can be different.

V. CONCLUSIONS

Z_n symmetry is a discrete symmetry that is not taken into account in current particle physics, since the plane wave approximation used to be postulated and can give nice result that agree well with experiment datas in most cases. But the non-plane-wave nature of particles has some non-negligible effects to collision of particles. For example, the so called ‘‘beam-size effect’’ is verified in experiments at the MD-1 detector on the VEPP-4 collider, Novosibirsk 1981 [49], which gives significant inconformity to standard QED calculation with plane wave approximation. Calculation of the same process with Gaussian type states get quite reasonable agreement with the experiment data [50]. By considering the non-plane-wave particle states, we can imagine particles exhibiting Z_n symmetry. How does this kind of symmetry behave after particle interaction remains to be unknown.

In this paper, we select a series of peculiar non-plane-wave fermion states which we call them ‘‘vortex fermion states with Z_n symmetry’’ to study behavior of Z_n symmetry in a simple example of muon decay. Z_n symmetry of this kind of states are constructed in momentum space and showed in coordinate space with some approximations. They are just special cases of the so called ‘‘spin-orbit states’’ which are extensively researched for recent years. We calculated the plane wave electron spectral-azimuthal distribution at certain emission angle after decay of muon in such state, which is only thing we can detect for muon decay. The result shows that the Z_n symmetry of initial state remains invariant after the decay process. Concretely, it is verified by the fact that electron distribution of final state displays the same Z_n symmetry as the initial vortex muon state do. Other interactions that share some similar features with the process we have considered in the paper may get the same result. Three selection rules are listed to specify these cases, though they can only cover a small part of all the interactions. So, the result may not represent general behavior of Z_n symmetry in particle interactions.

Though there is no realization of such kind of muon states nowadays, their photon version have been produced. And generation methods of electron and neutron versions have been proposed by some researchers. The methods should be generalized to muon and other fermions. The kind of vortex fermions provides a good stage for study Z_n symmetry in particle interactions. We hope that the study here can stimulate the relevant research both theoretically and experimentally.

ACKNOWLEDGMENTS

We thank the referee for careful reading and suggestions. This work was supported by grants of the National Natural Science Foundation of China (Grant No. 11975320) and the Fundamental Research Funds for the Central Universities, Sun Yat-sen University.

APPENDIX A: RELATIONS BETWEEN FERMION POLARIZATION PARAMETERS

We have two groups of parameters to describe polarization of plane wave fermions, i.e. $\alpha(\varphi_p)$, $\delta(\varphi_p)$ for spinor in Eq.(2) and a_p , b_p , c_p for polarization 4-vector in Eq.(4). They can be related to each other with one-to-one correspondence by three equations:

$$\cos \alpha(\varphi_p) = b_p \left(\frac{1}{\gamma} \cos^2 \theta_0 + \sin^2 \theta_0 \right) + a_p \sin \theta_0 \cos \theta_0 \left(\frac{1}{\gamma} - 1 \right), \quad (18)$$

$$\sin(\varphi_p - \delta(\varphi_p)) = \frac{c_p}{\sin \alpha(\varphi_p)}, \quad (19)$$

$$\cos(\varphi_p - \delta(\varphi_p)) = \frac{a_p \cos \theta_0 - b_p \sin \theta_0 + \cos \alpha(\varphi_p) \sin \theta_0}{\sin \alpha(\varphi_p) \cos \theta_0}, \quad (20)$$

where $0 < \alpha(\varphi_p) < \pi$ and $0 < \delta(\varphi_p) < 2\pi$. It can be got by short calculation according to definition of the two different polarization descriptions. For spinor case, combination of the two free angles (α , δ) gives spin direction \vec{s}_0 of plane wave state at its rest frame. For 4-vector case, a_p , b_p and c_p perform as weight factors of three orthogonal basis vectors at the moving frame, in which the 3-momentum of the state is \mathbf{p} . Detail calculation is showed as follows.

Under boosting from rest frame to moving frame with momentum p^μ , polarization 4-vector is changed from $s'_0 = (0, \mathbf{S}_0) = (0, a_0, b_0, c_0)$ to $s^\nu = (S^0, \mathbf{S}) = (S^0, a_p, b_p, c_p)$. For space part, only components that are parallel to the moving direction is changed (multiply by γ). We use two figures in Fig. 5 to calculate relations in the two frames. In

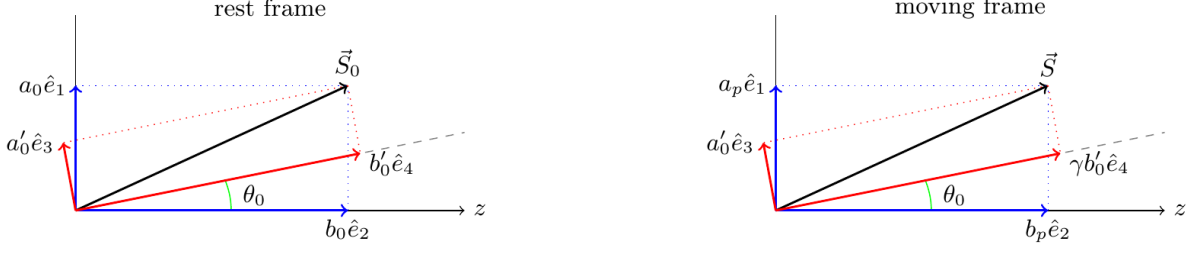


Figure 5. Polarization vector decomposition with different unit vectors (labeled as $\hat{e}_1, \hat{e}_2, \hat{e}_3$ and \hat{e}_4) in different reference systems. The plane we choose includes both \mathbf{p} and z axis. \vec{S}_0 and \vec{S} are projections of polarization vectors in the plane. Azimuthal component is vertical to the plane (not drawn) and do not change under boosting (i.e. azimuthal polarization projection keeps unchanged: $c_0 = c_p$). θ_0 corresponds to conical angle of vortex state.

the rest frame, we have

$$\vec{S}_0 = a_0 \hat{e}_1 + b_0 \hat{e}_2 = a'_0 \hat{e}_3 + b'_0 \hat{e}_4, \quad (21)$$

$$a_0 = a'_0 \cos \theta_0 + b'_0 \sin \theta_0, \quad (22)$$

$$b_0 = b'_0 \cos \theta_0 - a'_0 \sin \theta_0. \quad (23)$$

In the moving frame, we have

$$\vec{S} = a_p \hat{e}_1 + b_p \hat{e}_2 = a'_p \hat{e}_3 + \gamma b'_p \hat{e}_4, \quad (24)$$

$$a_p = a'_p \cos \theta_0 + \gamma b'_p \sin \theta_0, \quad (25)$$

$$b_p = \gamma b'_p \cos \theta_0 - a'_p \sin \theta_0. \quad (26)$$

We use angles to express unit vectors in different direction: $\mathbf{S}_0 \rightarrow (\alpha(\varphi_p), \delta(\varphi_p))$, $\hat{e}_1 \rightarrow (\pi/2, \varphi_p)$, $\hat{e}_2 \rightarrow (0, \varphi_p)$, $\hat{e}_3 \rightarrow (\theta_0 + \pi/2, \varphi_p)$, $\hat{e}_4 \rightarrow (\theta_0, \varphi_p)$, $\hat{e}_a \rightarrow (\pi/2, \varphi_p - \pi/2)$. Here $\hat{e}_a = \hat{e}_1 \times \hat{e}_2 = \hat{e}_3 \times \hat{e}_4$. Since

$$\mathbf{S}_0 \cdot \hat{e}_2 = \cos \alpha(\varphi_p), \quad (27)$$

$$\mathbf{S}_0 \cdot \hat{e}_1 = a_0 = a_p, \quad (28)$$

$$\mathbf{S}_0 \cdot \hat{e}_2 = b_0, \quad (29)$$

$$\mathbf{S}_0 \cdot \hat{e}_a = c_p, \quad (30)$$

we can directly get Eq.(18), and then Eq.(19) and Eq.(20) with all the equations given above. Polarization vector in the rest frame is normalized as $s_0^2 = -a_0^2 - b_0^2 - c_0^2 = -1$, which is Lorentz invariant. Thus, in the moving frame, we can get the normalization condition, i.e. Eq. (5), by calculation with equations given above.

APPENDIX B: IMPORTANT INTEGRALS USED IN SECTION IV

In section IV, we discussed result of integral showed in Eq. (17). We do not give accurate result but just give general features of different terms in the equation. All the discussions are based on some special integrals about trigonometric functions listed as follows. For any integers n and n' , if they are not equal, we have

$$\int_{\phi-\tau}^{\phi+\tau} d\varphi_p \cos n'(\varphi_p - \phi) \cos n\varphi_p = \frac{2(n' \cos n\tau \sin n'\tau - n \sin n\tau \cos n'\tau)}{n'^2 - n^2} \cos n\phi; \quad (31)$$

$$\int_{\phi-\tau}^{\phi+\tau} d\varphi_p \cos n'(\varphi_p - \phi) \sin n\varphi_p = \frac{2(n' \cos n\tau \sin n'\tau - n \sin n\tau \cos n'\tau)}{n'^2 - n^2} \sin n\phi; \quad (32)$$

$$\int_{\phi-\tau}^{\phi+\tau} d\varphi_p \sin n'(\varphi_p - \phi) \cos n\varphi_p = \frac{2(n' \sin n\tau \cos n'\tau - n \cos n\tau \sin n'\tau)}{n'^2 - n^2} \sin n\phi; \quad (33)$$

$$\int_{\phi-\tau}^{\phi+\tau} d\varphi_p \sin n'(\varphi_p - \phi) \sin n\varphi_p = \frac{2(n' \sin n\tau \cos n'\tau - n \cos n\tau \sin n'\tau)}{n^2 - n'^2} \cos n\phi. \quad (34)$$

If they are equal, we have

$$\int_{\phi-\tau}^{\phi+\tau} d\varphi_p \cos n(\varphi_p - \phi) \cos n\varphi_p = \frac{2n\tau + \sin 2n\tau}{2n} \cos n\phi; \quad (35)$$

$$\int_{\phi-\tau}^{\phi+\tau} d\varphi_p \cos n(\varphi_p - \phi) \sin n\varphi_p = \frac{2n\tau + \sin 2n\tau}{2n} \sin n\phi; \quad (36)$$

$$\int_{\phi-\tau}^{\phi+\tau} d\varphi_p \sin n(\varphi_p - \phi) \cos n\varphi_p = \frac{-2n\tau + \sin 2n\tau}{2n} \sin n\phi; \quad (37)$$

$$\int_{\phi-\tau}^{\phi+\tau} d\varphi_p \sin n(\varphi_p - \phi) \sin n\varphi_p = \frac{2n\tau - \sin 2n\tau}{2n} \cos n\phi. \quad (38)$$

When $\tau = \pi$, we just get the orthogonal theorem for integral of trigonometric functions.

- [1] G. L. Kotkin and V. G. Serbo, *Journal of Modern Physics A*. **7**, 4707-4745(1992).
- [2] D. V. Karlovets, *J. High Energ. Phys.* **2017**, 49(2017).
- [3] K. Y. Bliokh, I. P. Ivanov, G. Guzzinati, *et al*, *Physics Reports*. **690**, 1(2017).
- [4] V. Yu. Bazhenov, M. S. Soskin and M. V. Vashnetsov, *Journal of Modern Optics*. **39**, 985-990(1992).
- [5] M. W. Beijersbergen, L. Allen, H. E. L. O. van der Veen and J. P. Woerdman, *Optics Communications*. **96**, 123-132(1993).
- [6] L. Allen, M. W. Beijersbergen, R. J. C. Spreeuw and J. P. Woerdman, *Phys. Rev. A*. **45**, 8185(1992).
- [7] M. W. Beijersbergen, R. P. C. Coerwinkel and J. P. Woerdman, *Optics Communications*. **112**, 321-327(1994).
- [8] J. Bahrtdt, K. Holldack, P. Kuske, R. Müller, M. Scheer and P. Schmid, *Phys. Rev. Lett.* **111**, 034801(2013).
- [9] P. Liu, J. Yan, A. Afanasev, S. V. Benson, H. Hao, S. F. Mikhailov, V. G. Popov and Y. K. Wu, arXiv:2007.15723.
- [10] M. Uchida and A. Tonomura, *Nature*. **464**, 737-739(2010).
- [11] C. W. Clark, R. Barankov, M. G. Huber, M. Arif, D. G. Cory and D. A. Pushin, *Nature*. **525**, 504-506(2015).
- [12] A. Luski, Y. Segev, R. David, *et al*, *Science*. **373**, 1105(2021).
- [13] N. B. Simpson, K. Dholakia, L. Allen and M. J. Padgett, *Optics Letters*. **22**, 52-54(1997).
- [14] J. E. Curtis, B. A. Koss and D. G. Grier, *Optics Communications*. **207**, 169-175(2002).
- [15] K. Ladavac and D. G. Grier, *Optics Express*. **12**, 1144-1149(2004).
- [16] J. Leach, B. Jack, J. Romero, *et al*, *Science*. **329**, 662-665(2010).
- [17] J. Wang, J. Y. Yang, I. M. Fazal, *et al*, *Nature Photonics*. **6**, 488-496(2012).
- [18] J. Yuan, S. M. Lloyd and M. Babiker, *Physics*. **88**, 3181-3185(2013).
- [19] A. Konecna, M. K. Schmidt, R. Hillenbrand and J. Aizpurua, arXiv:2111.08810.
- [20] P. Schattschneider, V. Grillo and D. Aubry, *Ultramicroscopy*. **176**, 188-193(2017).
- [21] R. Juchtmans and J. Verbeeck, *Phys. Rev. A*. **93**, 023811(2016).
- [22] I. P. Ivanov and D. V. Karlovets, *Phys. Rev. Lett.* **110**, 264801(2013).
- [23] I. P. Ivanov, *Phys. Rev. D*. **83**, 093001(2011).
- [24] V. Serbo, I. P. Ivanov, S. Fritzsche, *et al*, *Phys. Rev. A*. **92**, 12705-12705(2015).
- [25] N. Dhankhar, S. Banerjee and R. Choubisa, *J. Phys. B: At. Mol. Opt. Phys.* **55**, 165202(2022).
- [26] R. V. Boxem, B. Partoens and J. Verbeeck, *Phys. Rev. A*. **89**, 032715(2014).
- [27] U. D. Jentschura and V. G. Serbo, *Eur. Phys. J. C*. **71**, 1-13(2011).
- [28] D. Seipt, A. Surzhykov and S. Fritzsche, *Phys. Rev. A*. **90**, 124-129(2014).
- [29] I. P. Ivanov, D. Seipt, A. Surzhykov and S. Fritzsche, *et al*, *Phys. Rev. D*. **94**, (2016).
- [30] A. Andrei, V. G. Serbo and S. Maria, *Journal of Physics G: Nuclear and Particle Physics*. **45**, 055102(2018).
- [31] A. V. Afanasev, D. V. Karlovets and V. G. Serbo, *Phys. Rev. C*. **100**, 051601(2019).
- [32] A. Afanasev and C. E. Carlson, *Phys. Rev. A*. **105**, 013522(2022).
- [33] P. Zhao, I. P. Ivanov and P. Zhang, *Phys. Rev. D*. **104**, 036003(2021).
- [34] M. A. A. Neil, F. Massoumian, R. Juskaitis and T. Wilson, *Optics Letters*. **27**, 1(2002).
- [35] C. Maurer, A. Jesacher, S. Furhapter, S. Bernet and M. Ritsch-Marte, *New Journal of Physics*. **9**, 78(2007).
- [36] J. Nsofini, D. Sarenac, C. J. Wood, *et al*, *Phys. Rev. A*. **94**, 013605(2016)
- [37] R. D. Romea and W. D. Kimura, *Phys. Rev. D*. **42**, 1807(1990).
- [38] P. Serafim, P. Sprangle and B. Hafizi, *IEEE Transactions On Plasma Science*. **28**, (2000).
- [39] B. Van Waeyenberge, A. Puzic, H. Stoll, *et al*, *Nature*. **444**, 461-464(2006).
- [40] E. Karimi, V. Grillo, R. W. Boyd and E. Santamato, *Ultramicroscopy*. **138**, 22-27(2014).
- [41] D. Sarenac, J. Nsofini, I. Hincks, *et al*, *New J. Phys.* **20**, 103012(2018).
- [42] D. Sarenac, C. Kapahi, W. Chen and D. A. Pushin, *PNAS*. **116**, 20328-20332(2019).
- [43] D. Sarenac, D. G. Cory, J. Nsofini, I. Hincks, P. Miguel, M. Arif, C. W. Clark, M. G. Huber and D. A. Pushin, *Phys. Rev. Lett.* **121**, 183602(2018).
- [44] V. B. Berestetskii, E. M. Lifshitz and L. P. Pitaevskii, *Quantum Electrodynamics* (China, Beijing, 2008).

- [45] U. D. Jentschura and V. G. Serbo, Phys. Rev. Lett. **106**, 013001(2011).
- [46] K. Y. Bliokh, M. R. Dennis, and F. Nori, Phys. Rev. Lett. **107**, 174802(2011).
- [47] V. Serbo, I. P. Ivanov, S. Fritzsche, D. Seipt, and A. Surzhykov, Phys. Rev. A. **92**, 012705(2015).
- [48] F. Andrew, M. de Oliveira and M. R. Dennis, Nature Photonics. **15**, 253–262 (2021).
- [49] A. E. Blinov, A. E. Bondar, Y. I. Eidelman, *et al*, Physics Letters B. **113B**, 423-6(1982).
- [50] V. N. Baier and V. M. Katkov, Phys. Rev. D. **66**, 053009(2002).